I. J. Trans. Phenomena, Vol. 8, pp. 331-344
Reprints available directly from the publisher
Photocopying permitted by license only

A Comparison of R245fa Pool Boiling Measurements to R123, and R245fa/Isopentane on a Passively Enhanced, Horizontal Surface

M. A. KEDZIERSKI*

National Institute of Standards and Technology
Bldg. 226, Rm B114
Gaithersburg, MD 20899

This study presents pool boiling heat transfer measurements for R245fa, R123 and a mixture of R245fa and isopentane on a flattened passively enhanced low-pressure boiling surface. Possibly because the enhanced surface was flattened from a round tube, its performance was sensitive to vapor seeding at start up. Consequently, the surface would operate in fully active and partially active boiling modes. The results indicate that the addition of 0.5 % mass isopentane to R245fa increases the heat flux by no more than 11 % greater than the heat flux of pure R245fa when the entire surface was actively boiling. By contrast, the heat flux of the R245fa/isopentane mixture was as much as 50 % greater than that of pure R245fa for a partially boiling-active surface. In addition, pure R123 pool boiling data was taken on the same passively enhanced surface that was used with R245fa and the mixture. The ratio of the pure R245fa heat flux to the pure R123 heat flux was independent of the fraction of the surface that was actively boiling. This is consistent with the hypothesis that isopentane acts to enhance the site density. That is, the addition of 0.5 % isopentane limits the heat transfer degradation that results from the loss of active sites by increasing the number of active sites in the actively boiling regions. From 8 kW/m^2 to 100 kW/m^2 and for fixed superheat, the R245fa heat flux was 27 % greater than that for R123. Considering only the boiling heat transfer characteristics of R245fa, it appears to be a good replacement for R123.

Keywords: Additive, Alternative refrigerants, Boiling, Enhanced heat transfer, R245fa, R123

INTRODUCTION

Currently HFC-R245fa (1,1,1,3,3-pentafluoropropane) serves primarily as a nonflammable and non-ozone depleting blowing agent alternative to HCFC-R141b for extruding low-density polyethylene (Williams et al., 1997, and Wu et al. 1999). Recently however, applications have arisen that require knowing the boiling characteristics of R245fa. For example, a major manufacturer has commercialized an R245fa organic Rankine cycle (Yana Motta, 2004). Zyhowski [2003] has shown that R245fa has the potential for greater efficiencies in an organic Rankine cycle as compared to HCFC-123 because of a more

*Corresponding Author: Phone: (301) 975-5282; Fax: (301) 975-8973

favorable sensible heating component. Another potential application for R245fa is as a working fluid in low-press water chillers for air-conditioning large buildings. There may be some incentive to replace the widely popular R123 as a low-press water chiller working fluid because R123 has a rather low, but non-zero (0.016) ozone depletion potential (ODP).

As of this writing, no major chiller manufacturer offers an R245fa chiller. One reason for this may be that an R245fa chiller will likely operate at presss that require press vessel construction. In addition, Zyhowski et al. [2002] states that the theoretical cycle efficiency of R245fa is less than that of R123 and proposes closing the gap between cycle efficiencies with multi-stage chillers. Consequently, there appears to be little opportunity for lowering power plant greenhouse gas emissions by switching from R123 to R245fa chillers. Despite these issues, R245fa is considered a viable alternative to R123 as a working fluid in chillers primarily because of it's zero ODP (Yana Motta, 2004).

One more reason for the absence of commercial R245fa chillers is the lack of component design data that can be used to optimize the performance and cost of R245fa chillers. The evaporator is a key element for the chiller. As such, the performance of the evaporator can strongly influence the efficiency of the chiller. Consequently, this paper presents pool boiling heat transfer data for R245fa referenced to that of R123 on the same heat transfer surface. In addition, and in an effort to possibly compensate for the lesser cycle performance of R245fa, this study compares the measured pool boiling heat transfer performance of pure R245fa to that of an R245fa/isopentane (99.5 % mass fraction/0.5 % mass fraction) mixture. The reason for this is that Kedzierski [1999, 2000] has shown that the boiling performance of refrigerants can be enhanced with hydrocarbon additives as briefly explained below.

Hydrocarbons in refrigerants can act similar to that of surfactants in water as a boiling augmentation. The main difference between the two is where

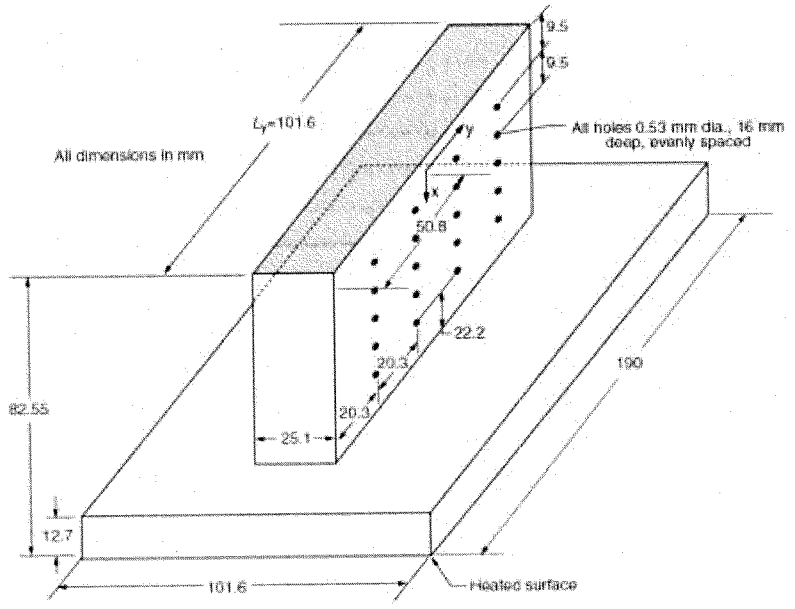

FIGURE 1
OFHC copper Turbo-BIII-LP test plate and thermocouple coordinate system.

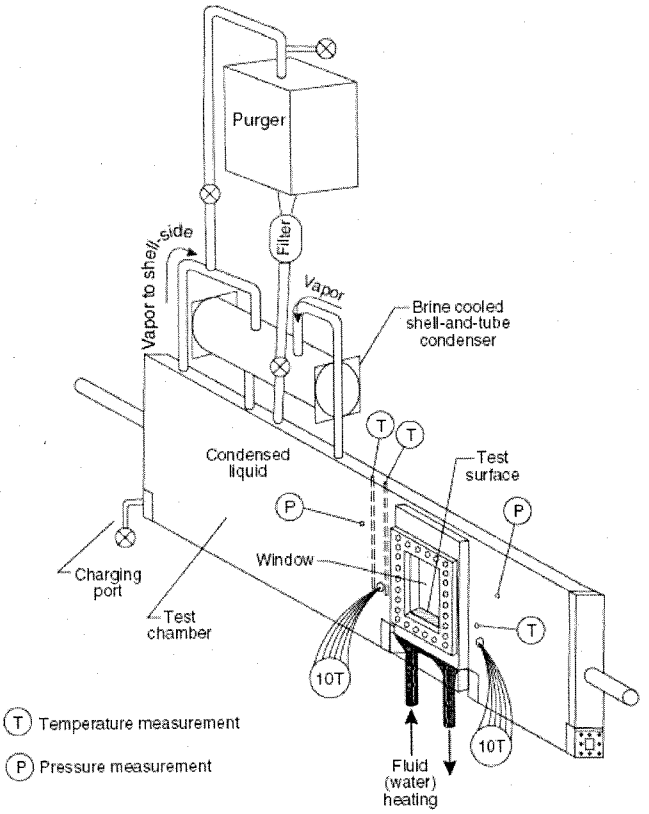

FIGURE 2
Schematic of pool boiling test apparatus.

the excess solute accumulates. The surfactant excess surface density in water resides at the liquid-vapor interface, while in general, the hydrocarbon excess surface density is at the liquid-solid interface. Both the surfactant and the hydrocarbon (as a dilute solute) cause a reduction in the bubble departure diameter by working on different force vectors on a bubble attached to the wall. This bubble diameter mechanism can enhance pool boiling heat transfer by increasing the active bubble site density (Kedzierski, 2001). A heat transfer enhancement exists when a favorable balance between an increase in site density and a reduction in bubble size occurs. In fact, Kedzierski [1999] measured a significant enhancement of R123 pool boiling with the addition of 1 % and 2 % hexane by mass to R123.

The pool boiling tests presented here for the three test fluids - R245fa, R123, and R245fa/isopentane (99.5/0.5) - were done on a flattened Turbo-BIII–LP* low-pressure boiling surface (see Fig. 1). The saturation temperature of each fluid was held at the design temperature of evaporators for chillers, which is approximately 277.6 K.

*Certain trade names and company products are mentioned in the text or identified in an illustration in order to adequately specify the experimental procedure and equipment used. In no case does such an identification imply recommendation or endorsement by the National Institute of Standards and Technology, nor does it imply that the products are necessarily the best available for the purpose.

APPARATUS

Figure 2 shows a schematic of the apparatus that was used to measure the pool boiling data of this study. Specifically, the apparatus was used to measure the liquid saturation temperature (T_s), the average pool-boiling heat flux (q''), and the wall temperature (T_w) of the test surface at the root of the fin. The three principal components of the apparatus were test chamber, condenser, and purger. The internal dimensions of the test chamber were 25.4 mm × 257 mm × 1.54 m. The test chamber was charged with approximately 7 kg of R245fa from the purger, giving a liquid height of approximately 80 mm above the test surface. As shown in Fig. 2, the test section was visible through two opposing, flat 150 mm × 200 mm quartz windows. The bottom of the test surface was heated with high velocity (2.5 m/s) water flow. The vapor produced by liquid boiling on the test surface was condensed by the brine-cooled, shell-and-tube condenser and returned as liquid to the pool by gravity.

The purger was used to remove non-condensable vapors from the refrigerant prior to testing. It was also used to store the entire liquid charge between tests. This was done to minimize the exposure of the elastomers to the liquid refrigerant in the event that they were not entirely compatible.

The mixture was prepared by first charging approximately 90 % of the R245fa into the test chamber to a known mass. Next, a measured mass of spectrophotometric grade isopentane was injected with a syringe through a valve in the side of the test chamber (see Fig. 2). The remaining R245fa charge was used to flush the valve and connecting tubes and also to assist in mixing the charge. The mass fraction was determined from the measured masses of the charged components. The maximum uncertainty of the mass fraction measurement is approximately 0.02 %, e.g., the range of the 0.5 % isopentane composition is between 0.48 % and 0.52 %.

TEST SURFACE

Figure 1 shows the oxygen-free high-conductivity (OFHC) copper Turbo-BIII–LP test plate and thermocouple coordinate system used in this study. Commercially, the Turbo-BIII–LP surface is rolled onto a smooth copper tube. A Turbo-BIII–LP copper tube was annealed, cut along the tube axis, and then soldered to the top of the test plate. The Turbo-BIII-LP surface has approximately 2362 fins per meter (fpm, 60 fins per inch (fpi)) oriented along the short axis of the plate.

MEASUREMENTS AND UNCERTAINTIES

The standard uncertainty (u_i) is the positive square root of the estimated variance u_i^2. The individual standard uncertainties are combined to obtain the expanded uncertainty (U), which is calculated from the law of propagation of uncertainty with a coverage factor. All measurement uncertainties are reported at the 95 % confidence level except where specified otherwise.

To reduce the errors associated with the liquid saturation temperature measurement, the saturation temperature of the liquid was measured with two 450 mm long, 1.6 mm diameter stainless steel sheathed thermocouples. The small diameter of the probes provided for a relatively rapid response time. Nearly the entire length of the thermocouple was in contact with either the test refrigerant vapor or liquid to minimize conduction errors. The tips of the two thermocouples were placed approximately 2 mm above and 150 mm (and 300 mm) to one side of the top of the test surface. This placement ensured that approximately 80 mm of the probe length was in relatively well-mixed liquid near the two-phase fluid above the test surface. To provide for a saturated liquid pool state, the mass of liquid in the pool was large compared to mass of liquid condensed. At the highest heat flux, it would require nearly 1 h to evaporate and condense the entire test chamber charge.

The copper-constantan thermocouples and the data acquisition system were calibrated against a glass-rod standard platinum resistance thermometer (SPRT) and a reference voltage to a residual standard deviation of 0.005 K. The NIST Thermometry Group calibrated the fixed SPRT to two fixed points having expanded uncertainties of 0.06 mK and 0.38 mK. A

quartz thermometer, which was calibrated with a distilled ice bath, agreed with the SPRT temperature to within approximately 0.003 K. Both the measured thermocouple electromotive force (EMF) and the measured 1 mV reference were regressed to the SPRT temperature. During a pool-boiling test, the 1 mV reference was measured prior to measuring each thermocouple EMF. The reference voltage was used to account for the drift in the acquisition measurement capabilities over time. Before each test run, the measurements of a thermocouple in the bath with the SPRT were compared. The mean absolute difference between the thermocouple and the SPRT was 0.06 K over one year. Considering the fluctuations in the saturation temperature during the test and the standard uncertainties in the calibration, the expanded uncertainty of the average saturation temperature was no greater than 0.04 K. Consequently, it is believed that the expanded uncertainty of the temperature measurements was less than 0.1 K. The saturation temperature was also obtained from a pressure transducer measurement with an uncertainty of less than 0.03 kPa. The uncertainty of the saturation temperature from a regression (with a residual standard deviation of 0.6 mK) of equilibrium data (Morrison and Ward, 1991) for R123 was 0.17 K. The saturation temperature obtained from the thermocouple and the pressure measurement nearly always agreed within ± 0.17 K for the pure R123 data.

Twenty 0.5 mm diameter thermocouples were force fitted into the wells of the side of the test plate shown in Fig. 2. The heat flux and the wall temperature were obtained by regressing the measured temperature distribution of the block to the governing two-dimensional conduction equation (Laplace equation). In other words, rather than using the boundary conditions to solve for the interior temperatures, the interior temperatures were used to solve for the boundary conditions following a backward stepwise procedure given in Kedzierski [1995]. Fourier's law and the fitted constants from the Laplace equation were used to calculate the average heat flux (q'') normal to and evaluated at the heat transfer surface based on its projected area. The average wall temperature (T_w) was calculated by integrating the local wall temperature (T). The wall superheat was calculated from T_w and the measured temperature of the saturated liquid (T_s). Considering this, the relative expanded uncertainty in the heat flux ($U_{q''}$) was greatest at the lowest heat fluxes, approaching 10 % of the measurement near 10 kW/m^2. In general, the $U_{q''}$ remained approximately within 3 % and 5 % for heat fluxes greater than 30 kW/m^2. The average random error in the wall superheat (U_{Tw}) was between 0.02 K and 0.1 K.

EXPERIMENTAL RESULTS

The heat flux was varied from approximately 125 kW/m^2 to 10 kW/m^2 to simulate a range of operating conditions for R245fa chillers equipped with enhanced tubes. All pool boiling tests were taken at 277.6 K ± 0.15 K saturated conditions.

The uncertainty in the temperature of the surface at the root of the fin was a function of the heat flux for the three test fluids on the Turbo-BIII–LP surface. The uncertainty in T_w was calculated from the regression of the solution to Laplace's equation. The uncertainties in the wall temperature are consistent from fluid to fluid increasing from approximately 0.045 K at 20 kW/m^2 to 0.09 K at 110 kW/m^2. The average random error in the wall superheat ΔT_s was within 0.1 K.

The relative uncertainty of the heat flux was also a function of the heat flux. Siu et al. [1976] estimated the uncertainty in the thermal conductivity of OFHC copper to be about 2 % to 3 % by comparing round-robin experiments. Considering this, the relative expanded uncertainty in q'' was greatest at the lowest heat fluxes, being between 4 % and 6 % at 20 kw/m^2. In general, the relative uncertainty of the heat flux remained within 3 % and 4 % for heat fluxes above 40 kW/m^2.

The data were recorded consecutively starting at approximately 125 kW/m^2 and then descending to 10 kW/m^2 in intervals of approximately 4 kW/m^2. The descending heat flux procedure was an attempt to minimize the possibility of any hysteresis effects, which would have made the data sensitive to the initial operating conditions. Despite these test procedure precautions, the pool boiling heat transfer

characteristics of the Turbo-BIII–LP surface exhibited a significant dependence on the initial number of cavities that held trapped vapor, i.e., the vapor seeding conditions. The sensitivity of the surface to what are believed to be initial (start up) operating may possibly be a result of the enhanced surface having been flattened from a round tube. The sensitivity from run to run caused the surface to operate in fully active and partially active boiling modes.

The ability/inability of the flat test specimen to become fully seeded may not be indicative of the vapor activity of a round tube. It is likely that a round tube may more readily become fully seeded from bubbles that slide within the fin channels, along the tube circumference, from the bottom to the top of the tube. Full vapor seeding may also be ensured for a chiller where the lower tubes provide vapor for the upper tubes. For these reasons, it is expected that round tubes in chillers may be much less sensitive to initial seeding condition.

This is not to say that pool boiling data from a tube and that from a flattened tube will never agree. On the contrary, this author's experience has been that the measured performance from a flattened tube compares closely to that of the round tube (e.g., Kedzierski, 1995). In addition, the significant extent to which the measurements from run to run are sensitive to start up heat flux has not been observed for flatten tubes until now. Typically, the heat flux beyond which the between run data becomes repeatable is much less than those observed in the present study. These behaviors may result from this particular surface having a greater requirement for the delivery of seed vapor to its cavities than other surfaces that have been tested.

The initial vapor seeding condition of the heat transfer surface was viewed through the two flat windows in the test apparatus as shown in Fig. 2. Sketches of the bubble activity on the surface were recorded in the laboratory book for each data point. Various fractions of the surface were observed to be active depending on the boiling regime and the heat flux experienced by the plate during startup of the test apparatus. The boiling regime was primarily established by the highest wall superheat experienced by the test plate. The largest heat flux to the test plate was dictated by the temperature difference between the water used to heat the test plate and the saturation temperature of the refrigerant. The saturation temperature of the refrigerant could not be easily controlled during the transient induced by test startup. Consequently, the largest heat flux experienced by the plate was approximated from the temperature of the heating water to the plate. The heat flux to the test plate was approximately 250 kW/m^2 when the water temperature was 340 K, which activated the entire plate with vigorous nucleate boiling.

Figure 3 shows a plot of the measured heat flux (q") versus the wall superheat (T_w - T_s) for pure R245fa. Data taken over six different days are shown on the figure. The open symbols represent tests where the entire surface appeared to be actively producing bubbles for the first recorded measurements at the highest heat flux. The fully active data are labeled as "good" vapor seeding in the key of the figure. The closed symbols represent tests where the surface was not completely active for the highest heat flux (labeled "poor" in the figure key). The estimated maximum heat flux that was experienced by the test surface is also given in the key. Tests for where the maximum heat flux was at or above 240 kW/m^2 corresponded to a fully active surface while tests where the maximum heat flux was estimated to be 100 kW/m^2 corresponded to a partially active test. The boiling curves for the partially inactive data are to the right of the fully seeded curves. The fully seeded data and the lowest heat transfer performance data were regressed and compared to the mixture data.

Figure 4 provides a plot of the measured heat flux (q") versus the wall superheat ($\Delta T_s = T_w - T_s$) for the R245fa/isopentane (99.5/0.5) mixture. Data from eight different test days are shown on the figure. At the largest heat flux, the test surface appeared to be fully active for all eight tests. However, the effect of initial seeding is evident by the variation in the boiling curve from day to day. It is believed that although the surface always appeared to be fully active, the days with the greater heat transfer resulted from the presence of additional bubbles that were not present on days when the heat transfer performance was less. This is plausible because the enhancement mecha-

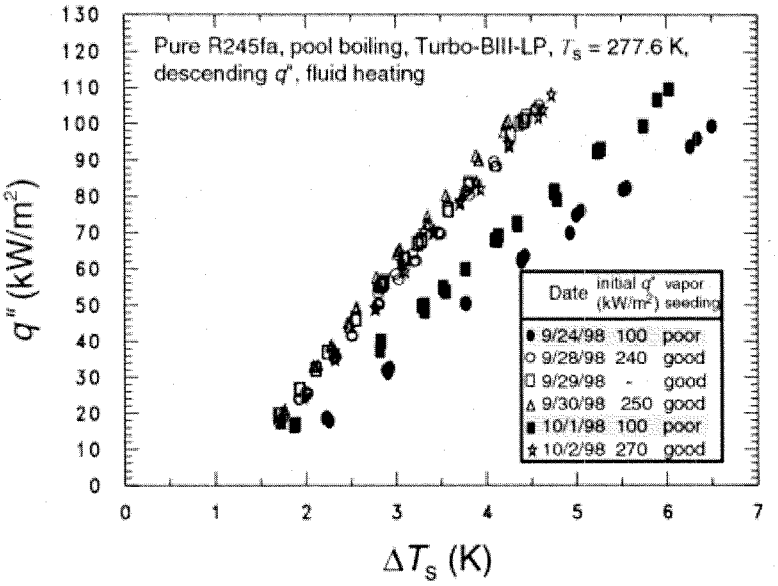

FIGURE 3
Pure R245fa pool boiling on Turbo-BIII-LP for fully and partially seeded data.

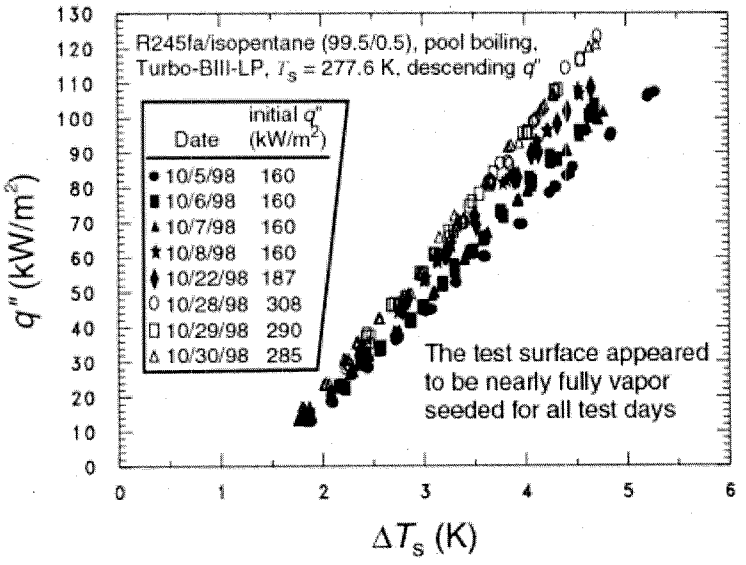

FIGURE 4
R245fa/isopentane (99.5/0.5) pool boiling on Turbo-BIII-LP.

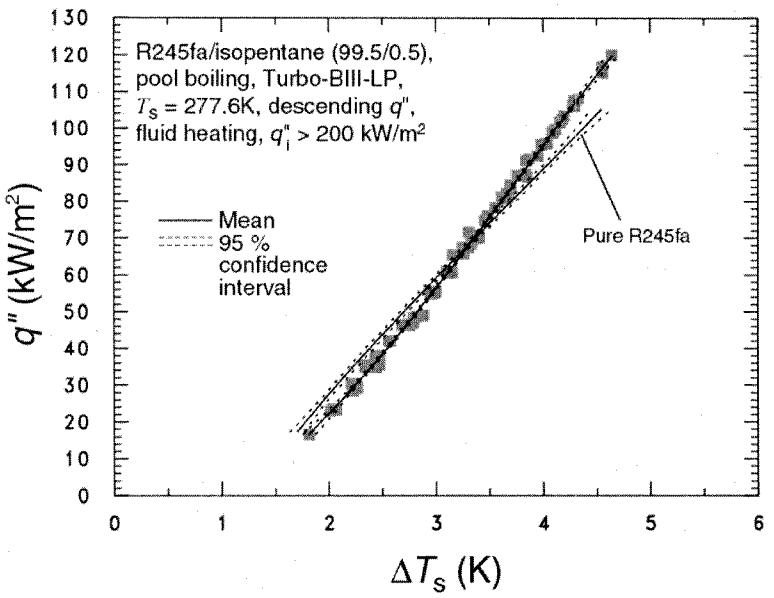

FIGURE 5
Pool boiling curve for R245fa/isopentane (99.5/0.5) on Turbo-BIII-LP surface (> 200 kW/m^2 data).

nism of a hydrocarbon additive for a refrigerant works by producing a greater site density with smaller bubbles when compared to the pure refrigerant (Kedzierski, 1999). It is likely that the fully seeded surface did not appear to differ with the addition of bubbles because they could not be seen with the naked eye. Consequently, the additional criterion for grouping test data was where the largest heat flux experienced by the test plate was above 200 kW/m$^{2(\dagger)}$. The open symbols represent tests where steam heating of the test plate water was used to elevate the initial heat flux above 200 kW/m^2. The closed symbols represent tests where initial heat flux to the test plate was below 200 kW/m^2. Although the entire test surface appeared to be uniformly active for every test day, the effect of initial heat flux on the boiling curve is still evident.

Figure 5 shows the pool boiling curve for the R245fa/isopentane (99.5/0.5) data for which the estimated initial heat flux exceeded 200 kW/m^2. The solid line is a cubic best-fit regression or estimated mean of the data. Table 1 gives the constants for the cubic regression of the superheat versus the heat flux for this and the other test fluids. The residual standard deviation of the regression - representing the proximity of the data to the mean – is 0.03 K. The dashed lines to either side of the mean represent the lower and upper 95 % simultaneous (multiple-use) confidence intervals for the mean. The expanded uncertainty of the estimated mean wall superheat is approximately 0.02 K.

Figures 6 and 7 illustrate the effect of the addition of 0.5 % mass isopentane to R245fa has on its boiling heat transfer performance. The Figures plot the ratio of the mixture to the pure R245fa heat flux (q''_m/q''_p) versus the pure R245fa heat flux (q''_p) at the same wall superheat. A heat transfer enhancement exists where the heat flux ratio is greater than one and the

[†]Due to the variation in the saturation pressure during start-up, the maximum heat flux is estimated based on the largest water temperature experienced by the test surface.

TABLE 1
Estimated parameters for cubic boiling curve fits for Turbo-BIII-LP.
$\Delta T_s = A_0 + A_1 q'' + A_2 q''^2 + A_3 q''^3$
ΔT_s in Kelvins and q'' in W/m^2

Fluid	A_o	A_1	A_2	A_3
R245fa (fully seeded) 1.5 K ≤ ΔT_s ≤ 5 K	1.25227	2.41220×10^{-5}	1.22710×10^{-10}	-5.20578×10^{-16}
R245fa/isopentane (99.5/0.5) (fully seeded) 1.5 K ≤ ΔT_s ≤ 5 K	1.20890	3.88054×10^{-5}	-1.60982×10^{-10}	6.37458×10^{-16}
R123 (fully seeded) 1.5 K ≤ ΔT_s ≤ 5 K	1.27954	5.030180×10^{-5}	-3.83265×10^{-10}	1.90596×10^{-15}
R245fa: 9/24/98 data (partially seeded with poorest Heat transfer performance) 2 K ≤ ΔT_s ≤ 6.5 K	1.34169	5.05095×10^{-5}	-1.08276×10^{-10}	1.32816×10^{-15}
R245fa/isopentane (99.5/0.5): 10/5/98 data (partially seeded with poorest Heat transfer performance) 2 K ≤ ΔT_s ≤ 5.5 K	1.41477	3.57513×10^{-5}	1.66193×10^{-11}	-1.54367×10^{-16}
R123: 9/18/98 data (partially seeded with poorest Heat transfer performance) 1.5 K ≤ ΔT_s ≤ 7.5 K	2.08124	4.75790×10^{-5}	-1.54750×10^{-10}	2.50350×10^{-15}

95 % simultaneous confidence intervals (depicted by dashed lines) do not include the value one. In . 6, comparison of the boiling performance of the pure R245fa and that of the mixture are made for only fully vapor-seeded data. Figure 7 compares low seeded data to low seeded data, i.e., the lowest performances for both fluids.

Figure 6 shows that the R245fa/isopentane (99.5/0.5) mixture exhibits an enhancement over pure R245fa for heat fluxes greater than approximately 72 kW/m^2. The maximum heat flux ratio for the 99.5/0.5 mixture was 1.11 at 120 kW/m^2. The average heat flux ratio for the R245fa/isopentane (99.5/0.5) mixture from 20 kW/m^2 to 120 kW/m^2 was 0.98. For 99.5 % confidence, no difference exists between the boiling performance of the 99.5/0.5 mixture and that for the pure R245fa for heat fluxes less than 20 kW/m^2. For the surface operating in the fully seeded condition, the additive would be useful only for heat fluxes above 72 kW/m^2. Otherwise, the addition of 0.5 % mass isopentane to R245fa could be detrimental to the boiling performance where the surface heat flux is below 72 kW/m^2. For example, the heat transfer performance for the mixture is approximately 83 % of that of pure R245fa at a heat flux of 30 kW/m^2.

Figure 7 compares the lowest heat transfer performance of the partial vapor seeded data for R245fa and R245fa/isopentane (99.5/0.5). The Figure shows that the R245fa/isopentane (99.5/0.5) mixture exhibits an enhancement for heat fluxes greater than approximately 12 kW/m^2. The maximum heat flux ratio for the 99.5/0.5 mixture was 1.5 ± 0.015 at 100 kW/m^2. The average heat flux ratio for the R245fa/isopentane (99.5/0.5) mixture from 10 kW/m^2 to 100 kW/m^2 was 1.33. The results suggest that the addition of 0.5 % mass isopentane to R245fa can be beneficial where the surface is not fully seeded. This is a consequence of the mixture data not exhibiting as much of a variation from the fully seeded to the partially seeded data as that which exists for the pure R245fa data (compare s. 3 and 4). Possibly the additive limits the inactivity of the surface via the site density enhancement mechanism.

Figure 8 provides a plot of the measured heat flux versus the wall superheat for pure R123. Data taken over ten different days are shown on the Figure. Open and closed symbols represent tests where the highest

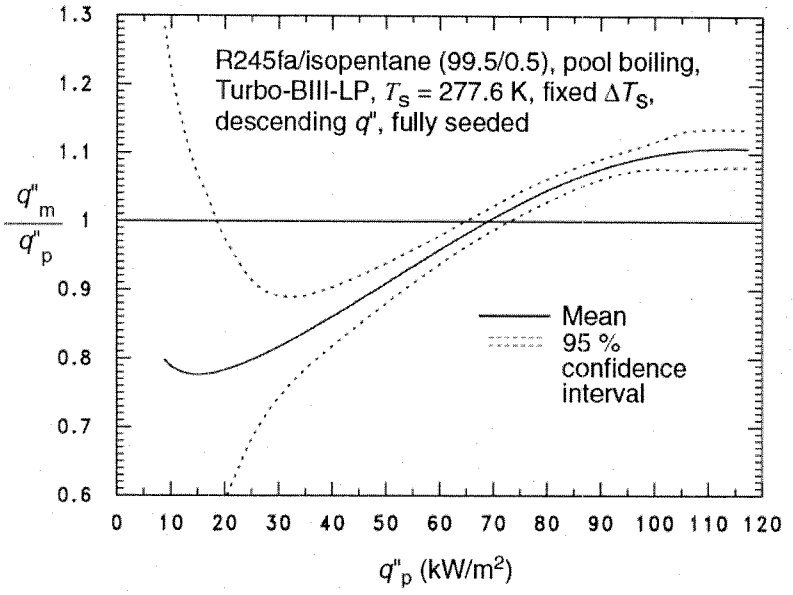

FIGURE 6
Heat flux ratio between R245fa/isopentane (99.5/0.5) and R245fa for fully seeded data.

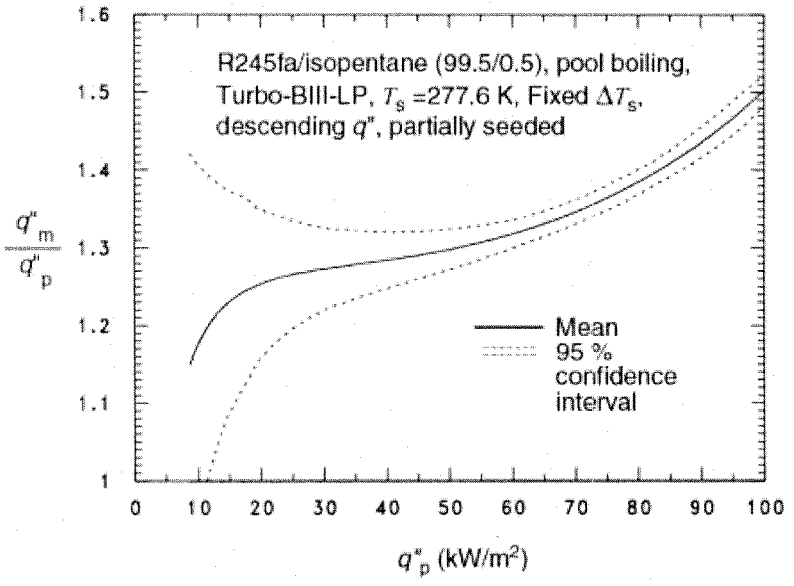

FIGURE 7
Heat flux ratio between R245fa/isopentane (99.5/0.5) and pure R245fa for low seeded data.

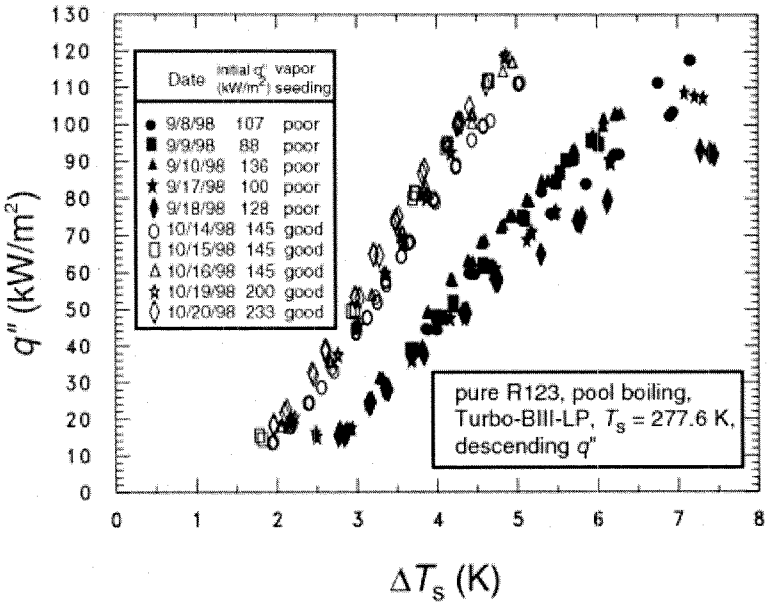

FIGURE 8
Pool boiling of R123 on TurboB-III-LP surface.

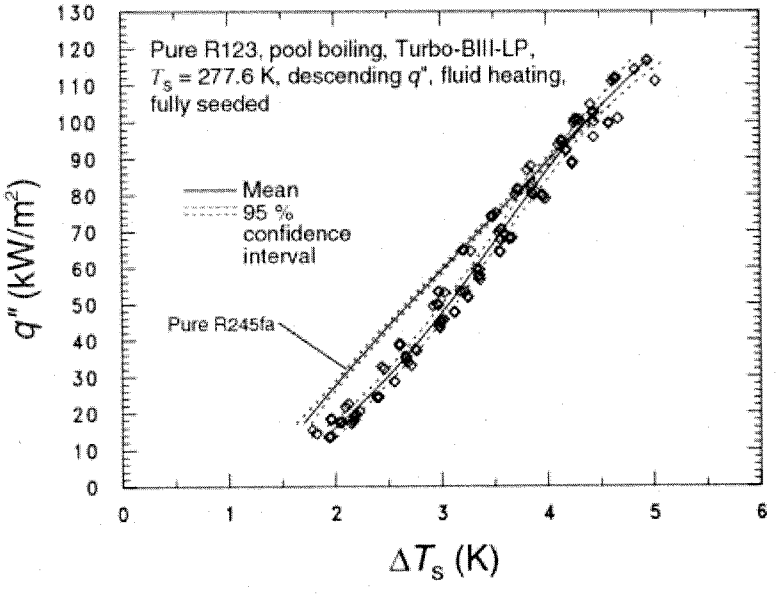

FIGURE 9
Pure R123 pool boiling on Turbo-BIII –LP.

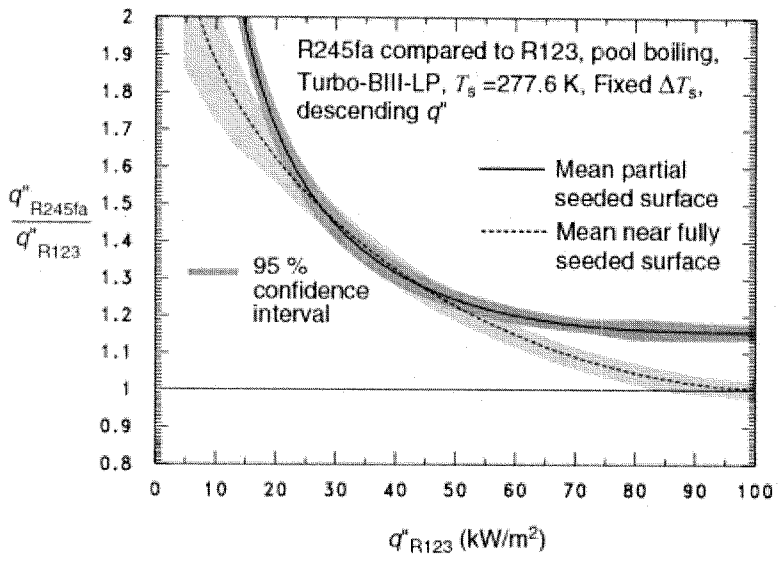

FIGURE 10
Relative boiling heat transfer of R245fa and R123 on TurboB-III-LP.

heat flux was approximately greater than 140 kW/m^2 and less than 140 kW/m^2, respectively. "Good" and "poor" are used to identify a fully active and a partially active heat transfer surface, respectively. The boiling curves for the partially inactive data are to the right of the fully seeded data and all corresponded to maximum heat fluxes less than 140 kW/m^2. The fully seeded data and the lowest heat transfer performance data were regressed and compared to the pure R245fa data.

Figure 9 shows the pool boiling curve for the pure R123 data for which the estimated initial heat flux exceeded 140 kW/m^2. The solid line is a cubic best-fit regression or estimated mean of the data. The residual standard deviation of the regression and the expanded uncertainty of the estimated mean wall superheat are approximately 0.12 K and 0.07 K, respectively. For comparison, the mean and confidence intervals of the fully seeded R245fa data is also given on the figure. The boiling performance of R245fa is greater than that of R123 for heat fluxes less than approximately 80 kW/m^2.

Figure 10 shows the relative boiling performance of R245fa to that of R123 for both fully seeded and partially seeded data. Inclusion of the 95 % confidence intervals for the partially seeded data mean is a bit misleading. For a fair comparison with the fully seeded data, the confidence interval for the partially seeded data should be increased because it does not include from run-to-run uncertainties. Because of this, it is likely that a difference between the relative boiling performance of R245fa and R123 for the two seeding conditions cannot be statistically discerned. Assuming that this is true, the relative performance curve of the fully seeded data is more reliable considering that it accounts for the uncertainties between runs. Consequently, only the relative performance for fully seeded will be discussed. For fully seeded condition, the pool boiling performance of R245fa exceeds that of R123 for heat fluxes less than approximately 83 kW/m^2. A heat flux ratio of approximately 1.6 ± 0.03 was observed at 22 kW/m^2. The heat flux ratio steadily decreased from 2 to 1 as the heat flux increased from 8 kW/m^2 to 100 kW/m^2. Averaged

over this heat flux range, the R245fa heat flux was 27 % greater than that of R123. The greater performance of R245fa can most likely be attributed to its higher reduced pressure (0.018) as compared to that of R123 (0.011) at the test temperature of 277.6 K. Considering only the boiling heat transfer properties of R245fa, it appears to be a good replacement for R123. This may allow designers to compensate somewhat for R245fa's theoretical lower thermodynamic efficiency as compared to that of R123.

CONCLUSIONS

The effect of the addition of 0.5 % by mass fraction isopentane to the boiling behavior of HFC-R245fa on a Turbo-BIII–LP surface was investigated. The magnitude of the enhancement depends on several factors including the number of surface cavities that retain seed vapor. Tests where the pure R245fa and the mixture appeared to have a fully active surface showed that the pool boiling heat flux of the R245fa/isopentane (99.5/0.5) mixture was no more than 11 % above the heat flux of pure R245fa. Conversely, tests where both fluids exhibited partially inactive surfaces indicated that 50 % enhancement of the heat flux was possible with the addition of 0.5 % mass isopentane to R245fa. Here, it is speculated that the degradation due to loss of seeding is limited for the R245fa/isopentane (99.5/0.5) mixture by the production of additional bubbles in the active boiling areas of the surface.

The enhancement of the R245fa pool boiling performance is also heat flux dependent. For the fully seeded condition, a heat transfer enhancement was observed between the range of 72 kW/m^2 and 120 kW/m^2; while a heat transfer degradation was observed for heat fluxes less than 72 kW/m^2. Although no degradation in the heat flux was observed for the partially seeded condition, the enhancement did increase with heat flux. On average, the mixture exhibited a 33 % greater heat flux than that of pure R245fa.

While the surface operates in the fully seeded condition, the additive would be useful only for heat fluxes above 72 kW/m^2. Otherwise, the addition of 0.5 % mass isopentane to R245fa could be detrimental to the boiling performance of R245fa where the heat flux is less than 72 kW/m^2. For example, the heat transfer performance for the mixture is approximately 83 % of that of pure R245fa at a heat flux of 30 kW/m^2.

The results suggest that the addition of 0.5 % mass isopentane to R245fa can be beneficial when the surface is not fully seeded. The enhancement is a consequence of the mixture data not exhibiting as much of a variation from the full seeded to the partially seeded data as that which exists for the pure R245fa data. Here, the isopentane acts to increase the site density in the active boiling areas, thus, limiting the degradation due to lack of vapor seeding.

In contrast to the R245fa/isopentane data, the ratio of the pure R245fa heat flux to the pure R123 heat flux was essentially independent of seeding condition. This is consistent with the hypothesis that isopentane acts to enhance the site density. From 8 kW/m^2 to 100 kW/m^2 and for fixed superheat, the R245fa heat flux was 27 % greater than that for R123. Considering only the boiling heat transfer properties of R245fa, it appears to be a good replacement for R123.

ACKNOWLEDGEMENTS

This work was jointly funded by NIST and The Trane Company (CRADA no. 1514) under Project Manager Dr. Shane Moeykens. Thanks go to the following people for their constructive criticism of the first draft of the manuscript: Dr. P. Domanski of NIST, C.J.L. Hermes of Multibras Appliances S.A. Brazil, and Dr. S. Yana Motta of Honeywell. The author would also like to express appreciation to Mr. G. Glaeser of the NIST Building Environment Division for data collection. Furthermore, the author extends appreciation to Mr. A. Heckert of the NIST Statistical Engineering Division for his consultations on the uncertainty analysis. Thanks also goes to Petur

Thors of Wolverine Tube, Inc. for donating the Turbo-BIII-LP surface for test.

NOMENCLATURE

English Symbols

A_n	regression constant in Table 1 n=0,1,2,3
q''	average wall heat flux, W/m^2
T	temperature, K
T_w	temperature at roughened surface, K
U	expanded uncertainty
u_i	standard uncertainty
y	test surface coordinate in Fig. 1, m
z	test surface coordinate in Fig. 1, m

English Subscripts

m	measured, mixture
p	pure
q"	heat flux
s	saturated state
Tw	wall temperature
w	wall or surface

Superscripts

-	average

REFERENCES

Eckert, E. R. G., and Goldstein, R. J., 1976. *Measurements in Heat Transfer*, Hemisphere, Washington, 2nd ed., pp. 9-11.

Kedzierski, M. A. (2001) The Effect of Lubricant Concentration, Miscibility and Viscosity on R134a Pool Boiling, *Int. J. Refrigeration*, Vol. 24, No. 4., pp. 348-366.

Kedzierski, M. A. (2000) Enhancement of R123 Pool Boiling by the Addition of Hydrocarbons, *Int. J. Refrigeration*, Vol. 23, pp. 89-100.

Kedzierski, M. A. (1999) Enhancement of R123 Pool Boiling by the Addition of N-Hexane, *Journal of Enhanced Heat Transfer*, Vol. 6, No. 5, pp. 343-355.

Kedzierski, M. A. (1995) Calorimetric and Visual Measurements of R123 Pool Boiling on Four Enhanced Surfaces, *NISTIR 5732*, U.S. Department of Commerce, Washington.

Kedzierski, M. A., and Worthington, J. L. III (1993) Design and Machining of Copper Specimens with Micro Holes for Accurate Heat Transfer Measurements, *Experimental Heat Transfer*, Vol. 6. pp. 329-344.

Morrison, G, and Ward, D. K. (1991) Thermodynamic Properties of Two Alternative Refrigerants: 1,1-Dichloro-2,2,2-Trifluoroethane (R123) and 1,1,1,2-Tetrafluoroethane (R134a), *Fluid Phase Equilibria*, Vol. 62, pp. 65-86.

Siu, M. C. I., Carroll, W. L., and Watson, T. W. (1976) Thermal Conductivity and Electrical Resistivity of Six Copper-Base Alloys, *NBSIR 76-1003*, U.S. Department of Commerce, Washington.

Williams, D. J., Bogdan, M. C., Parker, R. C., and Knopeck, G. M. (1997) Update on the Development of HFC-245fa as a Liquid HFC Blowing Agent, *J. of Cellular Plastics*, Vol. 33, pp. 238-363.

Wu, J., Albouy, A., and Mouton, D. (1999) Evaluation of the Next Generation HFC Blowing Agents in Rigid Polyurethane Foams, *J. of Cellular Plastics*, Vol. 35, pp. 421-437.

Yana Motta, S. (2004) Private communications, Honeywell Inc., Buffalo, N.Y.

Zyhowski, G. J. (2003) Opportunities for HFC-245fa Organic Rankine Cycle Appended to Distributed Power Generation Systems, *Proceedings of Int. Congress of Refrigeration*, ICR0508, Washington, DC.

Zyhowski, G. J., Spatz, M. W., and Yana Motta, S. (2002) An Overview of the Properties and Applications of Hfc-245fa, *Proceedings of the Int. Refrigeration and Air Conditioning Conference at Purdue*, paper R7-1.